

# Study on the Process Parameters of Cu-Cr-Zr Alloy Sample Prepared by Electron Beam Selective Melting

Zishan Lv, Ping Liu

University of Shanghai for Science and Technology, Shanghai 200093, China

---

## Abstract

In order to reduce the production cost of 3D printed copper alloy, Cu-Cr-Zr alloy powder prepared by atomization method was used as the raw material for electron beam selective melting (EBM) experiments. By optimizing the printing process parameters, almost completely dense Cu-Cr-Zr alloy block specimens were obtained, with a relative density of up to 99.99%. The microstructure of the prepared Cu-Cr-Zr alloy is fine equiaxed grains with Cr precipitation at the grain boundaries. Under quasi-static tensile conditions, its yield strength is  $(342 \pm 5)$  Mpa, tensile strength is  $(383 \pm 5)$  Mpa, and plastic deformation is  $22\% \pm 5\%$ . The comprehensive mechanical properties are almost consistent with the cast Cu-Cr-Zr alloy.

## Keywords

Additive Manufacturing; Metals and Alloys; Electron Beam; Mechanical Properties; Secondary Remelting.

---

## 1. Introduction

Additive Manufacturing technology is a suitable method to produce complex structure, individual parts and different parts. The additive manufacturing technology can adopt the optimized design scheme according to the application requirements, and is not restricted by the traditional manufacturing technology. In recent years, the application of pure copper and copper alloy in additive manufacturing has become more and more interesting, the development of blue or green diode laser sources (emission wavelengths  $\lambda = 450$  or  $515$  nm, respectively) for laser metal deposition has been shown to be effective in reducing the reflectivity of Cu to a reasonable 40%, increased process stability and efficiency [1], but electron beam powder layer melting (EB-PBF). EB-PBF is almost unaffected by the optical reflectivity of the material and thus has a high absorption (80%) during processing of pure copper and copper alloys, resulting in a dense sample[2-6]. Cu and Cu alloy is one of the most important metals in commercial application and consumption besides iron and aluminum, it is an ideal material for electronics, automobiles, and manufacturing of cooling walls for space engine combustion.

## 2. Material and Methods

The powder properties have great influence on the process parameters of EBM. The alloy powder was prepared by atomization of Cu-Cr-Zr alloy powder prepared by Jiangsu Weilali new material science and Technology Co., Ltd. The powder particle size is from 45 to 106 $\mu$ m. The content of powder elements is: Cr 0.50-1.50%, Zr 0.05-0.20%, and the rest is Cu. Experiments were performed on an EB-PBF system on the ARCAM EBM A2X device, The forming substrate adopts 170 \* 170 \* 30mm Cu alloy substrate to avoid stripping between the sample and the substrate. After molding, microscopic sections parallel to the molding direction and perpendicular to the molding direction were prepared. The metallographic sandpaper was ground to 7000 mesh and polished with the grinding paste of W0.5. The forming range of this instrument is 200 \* 200 \* 380mm, the electron beam power is 3000W,

the electron gun voltage is 60000V, and the electron beam point diameter is 250 μ m. Because the electron beam is used in the EBM process, the energy absorption rate of copper alloy printing can be greatly improved, up to nearly 80%, so as to obtain dense samples[8-11].Because the insufficient energy of a single scanning line will lead to insufficient interlayer binding and pore defects, but a single scanning line too much energy will lead to edge local overheating warping, some powder agglomeration form large melting droplets, has a great impact on the subsequent molding, so a single layer is scanned twice under low line energy.The process window is determined through the powder study: scanning speed 1800 ~ 2800 mm/s, beam flow 17 ~ 21 mA, line spacing 0.1 mm, focus deflection 10 mA, layer 50μm thick, linear energy is 0.429 ~ 0.667J / mm.

**Table 1.** Cu-Cr-Zr molding process parameters

Numble	Line energy (J/mm)	REL.Density (%)	Hardness(HV)
1	0.429	95.4	145.2
2	0.500	99.99	157.9
3	0.632	99.67	145.6
4	0.667	98.56	137.4
5	0.600	99.35	145.4
6	0.630	98.83	144.6
7	0.570	99.65	136.3
8	0.540	99.97	148.4
9	0.510	99.95	146.5

The line energy is calculated by formula (1). The line energy is related to P and v of the electron beam, and P is the product of UI. Hardness is adopted(HX-1000TM/LCD, Zwick Corporation, Germany)measure,REL.Density measured using the Archimedes drainage method, as formula (2),Where REL.Density is the actual density divided by the theoretical density.

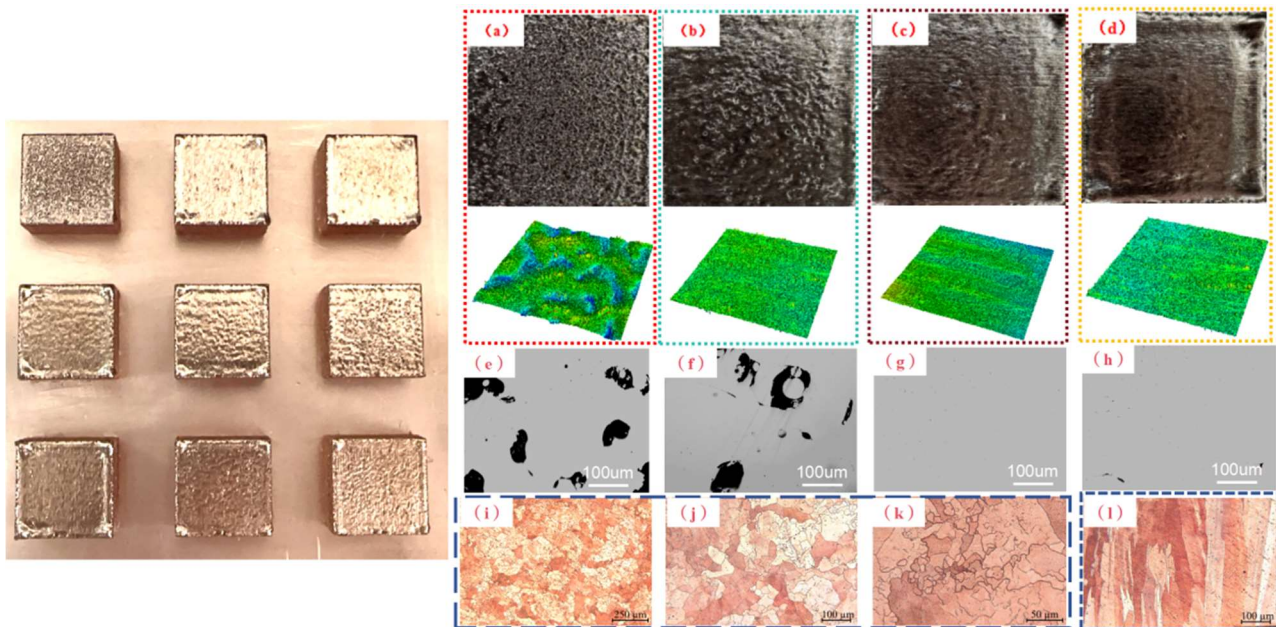
$$E_{\text{line}} = \frac{UI}{v} \tag{1}$$

$$\rho_{\text{rel.}} = \frac{\rho_{EB - PBF}}{\rho_{\text{standard}}} = \frac{\rho_{\text{water}} * m_{EBPBF(\text{air})}}{\rho_{\text{standard}} * (m_{EBPBF(\text{air})} - m_{EBPBF(\text{water})})} \tag{2}$$

### 3. Results and Discussion

Figure 1 shows the powder melting of the molded bulk samples in an EB-PBF machine. Figure 1 (a) (b) (c) (d) REL.density 95.4%, 97.83%, 99.99%, 99.65% of the sample surface amplification and scanning tunnel microscope, corresponding to table 1, line energy in 0.500~0.54J/mm, REL.Density above 99.9%, from figure 1 (a) (b) can be seen that the sample surface has more pores, no metallic luster, relatively rough, this is caused by insufficient line energy; The surface in Fig. 1(c) shows a metallic sheen and clear scanning lines,In Figure 1 (d), the melting pool boundary is unclear and the boundary is significantly expanded due to the large energy input. Too high line energy will lead to the instability of the melting pool.Figure 1 (e) (f) (g) (h) is the corresponding image of figure 1 (a) (b) (c) (d) samples under the optical microscope, (e) (f) can clearly see the surface pores, size is about 50~100 μ m, similar to the powder particle size, (g) almost no pores, (h) has a small amount of fine defects, may be generated by the melting pool lap.(I) (g) (k) for (c) and the molding direction of

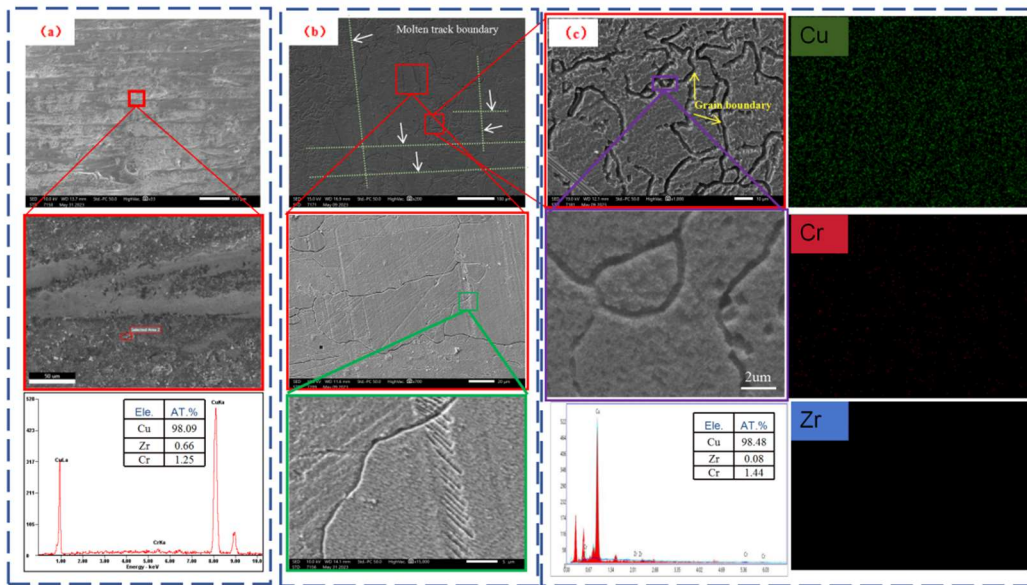
vertical corrosion micrograph, can see from the figure has many irregular grain, grain size in 10~100  $\mu$  m, but also have large grain, grain (l) for the molding direction of microscopic image, there are many slender column grain, grain growth along the sample forming direction through the multilayers, width of about 10~50  $\mu$  m, shorter and narrow column may be due to interlayer defects.



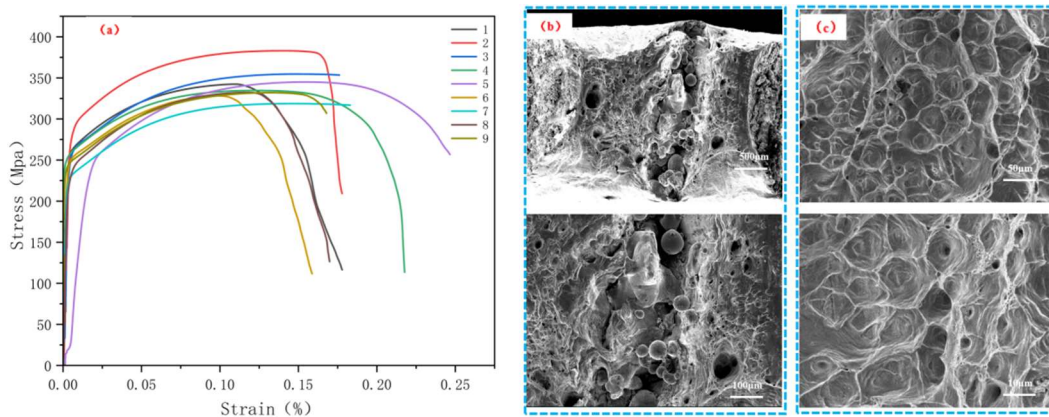
**Figure 1.** Sample diagram (left) ; (a) (b) (c) (d) is the surface topography amplification map of the corresponding REL. density 95.4%, 97.83%, 99.99%, 99.65% samples and the images taken by the scanning tunnel microscope; (e) (f) (g) (h) corresponding to (a) (b) (c) (d); (i) (j) (k) (l) is the microscopic image after (c) corrosion in the transverse and vertical direction.

Figure 2 (a) is the SEM image on the surface of Cu-Cr-Zr alloy, corresponding to the samples in Figure 1 (c), has a clear molten pool morphology, the surface almost no defects, due to the interlayer rotation 90, can see that the molten pool of different layers, remelt the former layer, the amplified area EDS elements in Figure 2 (a) analysis results can see the elements on the alloy surface distribution uniform, and there is no element agglomeration, Zr element content at the boundary of the molten pool. Figure 2 (b) (c) shows the obvious crystal boundary, and the EDS elements are evenly distributed, because the Zr element content is small, so it is almost undetectable.

The tensile stress and strain curves of the Cu-Cr-Zr alloy prepared by SEBM are shown in Figure 3 (a). Its tensile strength was 383 Mpa, yield strength was 294 Mpa and elongation was 17.6%. This is because the SEBM shaping process is a rapid melting and solidification process. During the solidification process, due to the rapid cooling rate, the nucleation of the grain has no time to grow, thus obtaining the fine grain organization. To further investigate the fracture mechanism, the fracture morphology of the Cu-Cr-Zr samples prepared by SEBM is shown in Figure 3 (b) (c). As shown in Figure 3 (b) for the fracture image of No.1 sample, there are large defects on the fracture surface, which is due to the low interlayer energy density and the formation of irregular holes and defects, it is obvious to see the unmelted powder in the fracture. Figure 3 (c) shows the fracture image of sample No.2. It can be seen that many large and deep toughness nests are evenly distributed on the surface of the sample fracture, and many smaller toughness nests are distributed around the large ones, showing the characteristics of toughness fracture.



**Figure 2.** (a)SEM image of Sample surface(b)The SEM images after the corrosion(c)EDS elemental analysis.



**Figure 3.** (a) Stress-strain curve of SEBMed CuCrZr, (b) SEM images of the fracture surface of tensile No.1 , and (c) the morphology of sample 2.

#### 4. Conclusion

In this paper, the influence of process parameters on SEBM compaction behavior and microorganization characteristics of Cu-Cr-Zr alloy was systematically investigated. The process parameters of Cu-Cr-Zr alloy were optimized by secondary remelting, and the microorganization and mechanical properties of the optimized Cu-Cr-Zr alloy were characterized. The main conclusions of this paper are summarized as follows: The feasibility of the secondary remelting scheme was confirmed and the process window was determined with the sample REL. density above 99.9% at the line energy of 0.500J/mm~0.540J/mm. When the energy density is low, the surface defects are very obvious, the powder adhesion on the surface, and the high energy density will also affect the performance of the molding part, which will lead to surface warping. Under the optimal parameters, the hardness of the sample reaches 157.9HV and the elongation rate reaches 17.6%. In the future, the samples prepared by SEBM will be further explored for thermal conductivity and conductivity.

## References

- [1] E. Martinez, D.A. Ramirez, L.E. Murr. Novel precipitate-microstructural architecture developed in the fabrication of solid copper components by additive manufacturing using electron beam melting (Article)[J]. *Acta Materialia*, 2011, Vol. 59(10): 4088-4099.
- [2] Y. Sato, M. Tsukamoto, T. Shobu, Y. Funada, Sakon, et al. In situ X-ray observations of pure-copper layer formation with blue direct diode lasers. [J]. *Applied Surface Science*, 2019, Vol. 480(1): 861-867.
- [3] Lodes, M.A., Guschlbauer, R., Körner, C. Process development for the manufacturing of 99.94% pure copper via selective electron beam melting (Article)[J]. *Materials Letters*, 2015, Vol. 143: 298-301.
- [4] Guschlbauer, R., Momeni, S., Osmanlic, F., Körner, C. Process development of 99.95% pure copper processed via selective electron beam melting and its mechanical and physical properties [J]. *Materials Characterization*, 2018, Vol. 143: 163-170.
- [5] Raab, S. J., Guschlbauer, R., Lodes, M. A., Körner, C. Thermal and electrical conductivity of 99.9% pure copper processed via selective electron beam melting [J]. *Advanced Engineering Materials*, 2016, Vol. 18(9): 1661-1666.
- [6] Ralf Guschlbauer, Pär Arumskog, Simon Eichler. Electron Beam Melting of Pure Copper - From Research to Industrialization [A]. 2020 IEEE 21st International Conference on Vacuum Electronics (IVEC) [C], 2020.
- [7] Zuo Wei, Song Menghua, Yang Huanqing, Chen Xinhong. Application of additive manufacturing technology in liquid rocket engine [J]. *Journal of Rocket Propulsion*, 2018, Vol. 44(2): 55-65.
- [8] Yue, Mingkai, Li, Meie, An, Ning, Yang, Kun, Wang, Jian, Zhou, Jinxiong. Modeling SEBM process of tantalum lattices [J]. *RAPID PROTOTYPING JOURNAL*, 2023, Vol. 29(2): 232-245.
- [9] Ordás N, Portolés L, Azpeleta M, et al. Development of CuCrZr via electron beam powder bed fusion (EB-PBF) [J]. *Journal of Nuclear Materials*, 2021, 548: 152841.
- [10] Wallis C, Buchmayr B. Effect of heat treatments on microstructure and properties of CuCrZr produced by laser-powder bed fusion [J]. *Materials Science and Engineering: A*, 2019, 744: 215-223.
- [11] Terrazas C A, Gaytan S M, Rodriguez E, et al. Multi-material metallic structure fabrication using electron beam melting [J]. *The International Journal of Advanced Manufacturing Technology*, 2014, 71: 33-45.